Heparan sulfate proteoglycans: key moderators of the interaction of multiple myeloma with the bone marrow niche

Ren, Z.

[Link to publication](#)

Aberrantly expressed LGR4 empowers Wnt signaling in Multiple Myeloma by hijacking osteoblast-derived R-spondins

Harmen van Andel[1,2], Zemin Ren[1,2], Iris Koopmans[1,2], Sander P.J. Joosten[1,2], Kinga A. Kocemba[1,2,3], Wim de Lau[4], Marie José Kersten[2,5], Alexander M. de Bruin[1,2], Jeroen E.J. Guikema[1,2], Hans Clevers[4], Marcel Spaargaren[1,2,6] and Steven T. Pals[1,2,6]

[1]Department of Pathology, Academic Medical Center, University of Amsterdam, Amsterdam, The Netherlands; [2]Lymphoma and Myeloma Center Amsterdam – LYMMCARE, Amsterdam, The Netherlands; [3]Department of Medical Biochemistry, Jagiellonian University Medical College, Poland; [4]Hubrecht Institute, Utrecht, The Netherlands and [5]Department of Hematology, Academic Medical Center, University of Amsterdam, Amsterdam, The Netherlands; [6]The authors share last authorship

Abstract

The unrestrained growth of tumor cells is generally attributed to mutations in essential growth control genes, but tumor cells are also affected by, or even addicted to, signals from the microenvironment. As therapeutic targets, these extrinsic signals may be equally significant as mutated oncogenes. In multiple myeloma (MM), a plasma cell malignancy, most tumors display hallmarks of active Wnt signaling but lack activating Wnt-pathway mutations, suggesting activation by autocrine Wnt ligands and/or paracrine Wnts emanating from the bone marrow (BM) niche. Here, we report a pivotal role for the R-spondin/LGR4 axis in driving aberrant Wnt/β-catenin signaling in MM. We show that LGR4 is expressed by MM plasma cells, but not by normal plasma cells or B cells. This aberrant LGR4 expression is driven by IL-6/STAT3 signaling and allows MM cells to hijack R-spondins produced by (pre) osteoblasts in the BM niche, resulting in Wnt (co-)receptor stabilization and a dramatically increased sensitivity to auto- and paracrine Wnts. Our study identifies aberrant R-spondin/ LGR4 signaling, with consequent deregulation of Wnt (co-) receptor turnover, as a driver of oncogenic Wnt/β-catenin signaling in MM cells. These results advocate targeting of the LGR4/R-spondin interaction as a therapeutic strategy in MM.

Introduction

Multiple myeloma (MM) is an in most patients incurable hematologic malignancy characterized by the accumulation of clonal plasma cells in the BM. Despite the wide variety of underlying structural and numerical genomic abnormalities[1-3], virtually all MMs are highly dependent on a protective BM microenvironment, or 'niche', for growth and survival.[4] Understanding the complex reciprocal interaction between MM cells and the BM microenvironment is critical for the development of new targeted therapies.

In MM, aberrant activation of the canonical Wnt pathway drives proliferation and is associated with disease progression, dissemination, and drug resistance.[5-9] Since MMs with hallmarks of active Wnt signaling do not harbor mutations that typically underlie constitutive Wnt pathway activation, this oncogenic Wnt pathway activity was proposed to involve autocrine and/or paracrine Wnt ligands.[6,8,10] Wnts are lipid-modified glycoproteins that function as typical niche factors since they are relatively unstable and insoluble due to their hydrophobic nature, which constrains long-range signaling.[11] Binding of a Wnt ligand to its receptor Frizzled (Fzd) initiates a signaling cascade that ultimately results in stabilization and nuclear translocation of the Wnt effector β-catenin. In cooperation with TCF/LEF family transcription factors this orchestrates a transcriptional program,[12,13] comprising targets such as c-Myc and Cyclin D1 that play crucial roles in the pathogenesis of MM.[14-16] Aberrant Wnt signaling in cancer typically results from mutations in *APC*, β-catenin (CTNNB1), or *AXIN* that drive constitutive, ligand-independent pathway activation.[10] Interestingly, mutations in regulators of Wnt receptor turnover, causing hypersensitivity to Wnt ligands, have recently been described in a variety of tumors, identifying aberrant Wnt (co-)receptor turnover as an alternative mechanism driving oncogenic Wnt signaling.[17-19] Turnover of Wnt (co-)receptors is critically regulated by LGR-family receptors, which stabilize Wnt (co-)receptors in response to their cognate ligand R-spondin. R-spondin/LGR signaling alleviates the inhibitory effect of two homologous membrane-bound E3 ubiquitin-ligases, ZNRF3 and RNF43, which normally induce Wnt (co-)receptor internalization.[20-23] This strong positive regulatory effect on Wnt signaling pathway activation designates the LGR/R-spondin axis as potentially oncogenic, a notion that prompted us to explore its possible role in hematologic malignancies. Here, we identify aberrant LGR4/R-spondin signaling as a driver of oncogenic Wnt/β-catenin signaling in MM.

2

Results

LGR4 is aberrantly expressed in MM

To gain insight into the expression of *LGR4-6* in normal hematopoiesis and in hematologic malignancies, we initially analyzed publically available gene-expression data sets. In normal bone marrow and lymphocyte subsets, as well as in most hematologic malignancies, *LGR4-6* mRNA was virtually undetectable. (Fig 1 and Fig. S1A). Interestingly, however, *LGR4* expression was present in the majority of primary MMs (pMMs) (Fig 1) at levels comparable to those in intestinal tissues (Fig S1B), in which the role of LGR/R-spondin signaling is well established.[24] No significant differences in *LGR4* expression were observed between MMs from previously defined molecular subgroups (Fig. S1C).[25] Notably, no significant expression of *LGR5* or *LGR6* was detected in MM samples (Fig.S1D). qPCR analysis confirmed *LGR4* mRNA expression in most human multiple myeloma cell lines (HMCLs) and pMMs (Fig 2A). In contrast, *LGR4* mRNA was virtually absent in normal B-cell subsets, *i.e.*, naïve B cells (CD19$^+$/IgD$^+$/CD38$^-$), pre-germi-nal center B cells (pGC, CD19$^+$/IgD$^+$/CD38$^+$), germinal center B cells (GC, CD19$^+$/IgD$^-$/CD38$^+$), memory B cells (CD19$^+$/IgD$^-$/CD38$^-$) and plasmablasts (CD19$^+$/IgD$^-$/CD38^{hi}) isolated from tonsils (Fig 2A). No *LGR5* and *LGR6* mRNA was detected in pMM, HMCLs and developing B cells by qPCR (Fig. S2A). In agreement with the mRNA data, flow cytometric analysis employing an LGR4-specific monoclonal antibody (mAb) (Fig. S2B) revealed that LGR4 protein is expressed on the majority of pMMs and HMCLs (Fig. 2B-D) but, importantly, not on normal bone mar-row derived plasma cells (hBMPCs) (Fig. 2B) or normal B-cell subsets (Fig. S2C). LGR5 protein expression was not detected in pMMs and HMCLs (Fig. S2D). These findings indicate that LGR4 expression in MM is a hallmark of malignant transformation and not a reflection of differentia-tion status or lineage commitment.
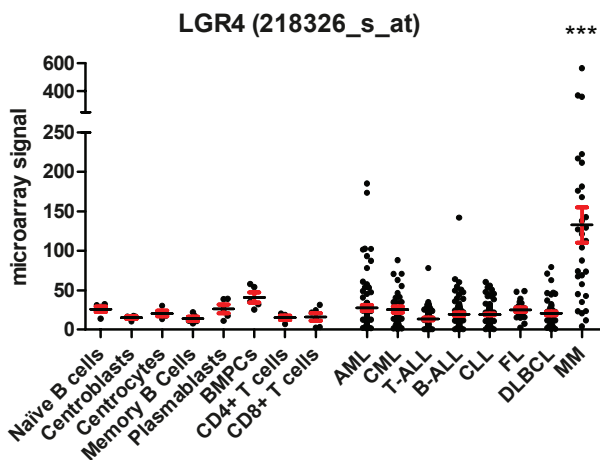
Fig. 1. LGR4 expression in normal hematopoiesis and hematologic malignancies.
Analysis of LGR4 mRNA expression in publically available microarray datasets. AML: acute myeloid leukemia; B-ALL: B-cell acute lymphoblastic leukemia; BMPC: bone marrow plasma cells; CLL: chronic lymphoid leukemia; CML: chronic myeloid leukemia; DLBCL: diffuse large B-cell lymphoma; FL: follicular lymphoma; T-ALL: T-cell acute lymphoblastic leukemia. Data were normalized by global scaling to 100. ***P ≤ 0.001 using one-way ANOVA with Bonferroni correction.

Fig. 2. LGR4 is expressed in MM plasma cells, but not in normal plasma cells or B-cell subsets.
(A) LGR4 mRNA expression in HEK293T cells, normal B-cell subsets (n = 5), pMMs (n = 4), and HMCLs (n = 9), analyzed by qPCR and normalized to TBP. (B) LGR4 protein expression in hBMPCs and pMMs. (C) Quantification of geometric mean of LGR4 FACS stainings in hBMPC (n = 4) and MM (n = 12) samples. Unpaired Student's t-test with Mann–Whitney correction was used for statistical analysis; **P ≤ 0.01. (D) LGR4 protein expression in control transduced (black) or CRISPR/CAS9-mediated LGR4 KO HMCLs (red).
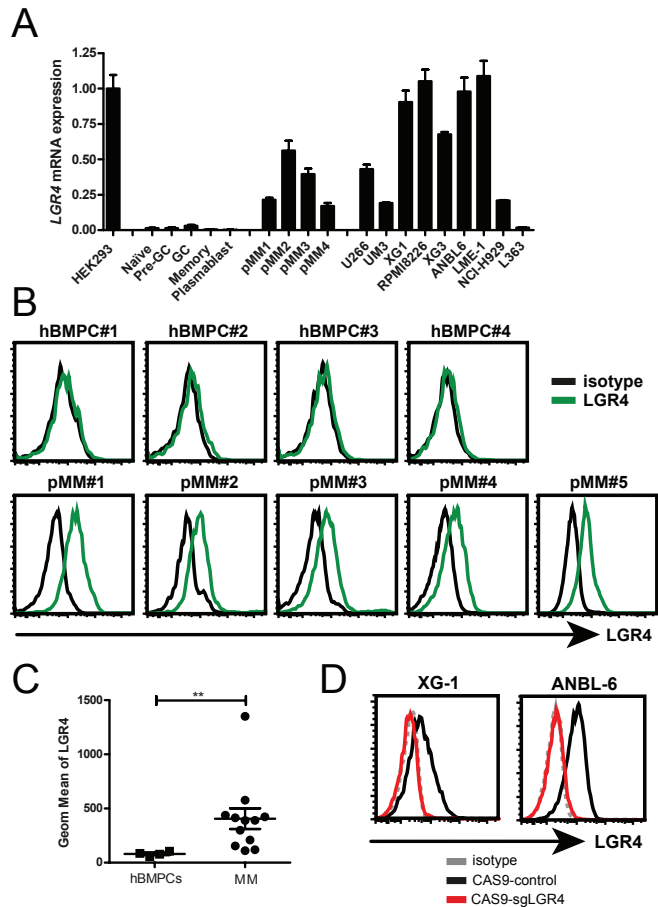
LGR4 expression is transcriptionally regulated by STAT3 signaling

STAT3 signaling is almost invariably activated in MM as a result of auto- or paracrine stimulation by IL-6[26-28], and was recently shown to regulate LGR4 expression in osteosarcoma.[29] We therefore investigated whether STAT3 signaling also mediates aberrant LGR4 expression in MM. As expected, IL-6 treatment of the HMCL XG-1 and pMM cells induced phosphorylation of the tyrosine 705 residue of STAT3, indicating pathway activation (Fig. S3A/B). Interestingly, IL-6 treatment of HMCLs and pMM cells, and ectopic expression of a constitutive active (CA) STAT3 mutant in XG-1, induced robust LGR4 mRNA and protein expression (Fig. 3 and S3B/C). Conversely, inhibition of STAT3 signaling, either by inducible shRNA-mediated silencing of STAT3 or ectopic expression of a dominant negative STAT3 mutant (DN-STAT3), significantly decreased both base-line and IL-6-induced LGR4 expression (Fig. 3B and S3D/E). Taken together, these findings indicate that STAT3 signaling instigates aberrant LGR4 expression in MM.

Fig. 3. LGR4 expression in MM is under transcriptional control of STAT3 signaling. (**A**) qPCR for LGR4 mRNA (Top) and flow cytometry analysis of LGR4 (Bottom) in three pMMs treated with or without IL-6 for 24 h. Error bars indicate ± SEM of three independent experiments; **P ≤ 0.01 and ***P ≤ 0.001 using unpaired Student's t-test. (**B**) Flow cytometry analysis of LGR4 in XG-1 cells treated with or without IL-6 (Left), transduced with CA-STAT3 (Middle), or transduced with DN-STAT3 (Right).
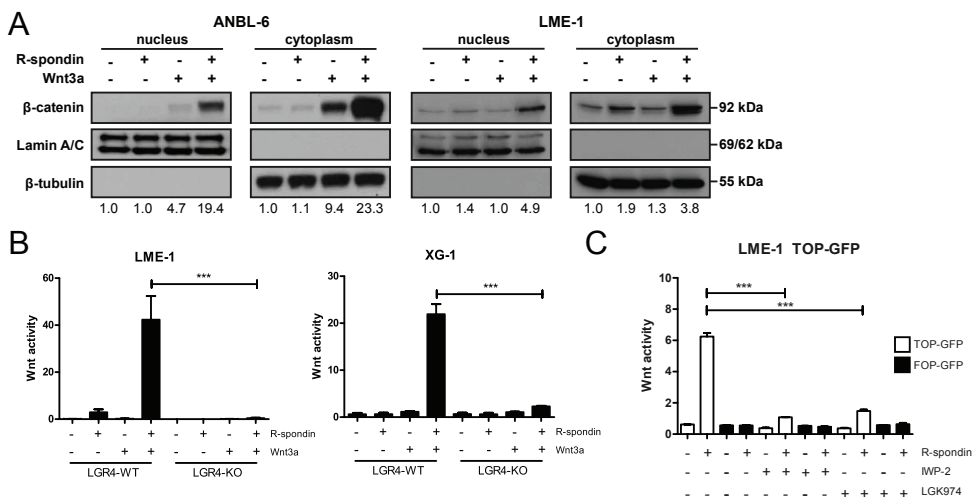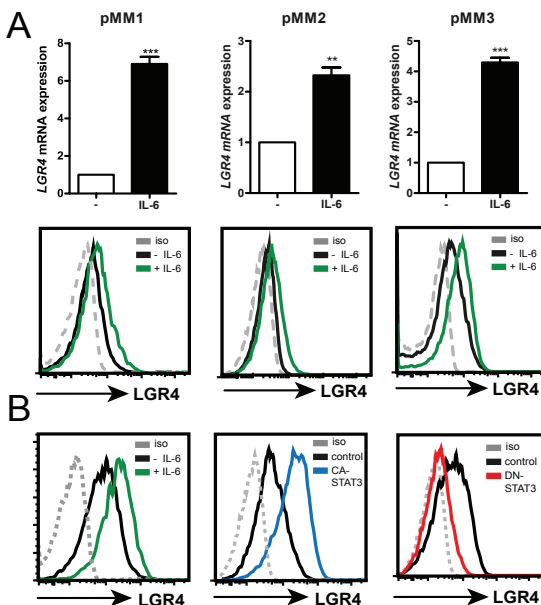

Fig. 4. R-spondins potentiate Wnt/β-catenin signaling in MM in an LGR4-dependent manner.
(A) Analysis of subcellular distribution of β-catenin in HMCLs after treatment with recombinant R-spondin 2, Wnt3a, or both by Western blot is representative of five independent experiments. β-Tubulin (cytoplasm) and lamin A/C (nucleus) served as fractionation and loading controls. Densitometric quantification (β-catenin/lamin A/C for nuclear fractions and β-catenin/β-tubulin for cytoplasmic fractions) relative to unstimulated conditions is shown below. (B) Flow cytometry analysis of Wnt activity in TOP-GFP–transduced HMCLs treated with R-spondin 2, Wnt3a, or both after CRISPR/CAS9-mediated LGR4 KO. Wnt activity is plotted as the percentage of mCherry/TOP-GFP double positive live cells. Error bars indicate ± SEM of three independent experiments in triplicate; ***P ≤ 0.001 using one-way ANOVA with Bonferroni correction. (C) Flow cytometry analysis of Wnt activity in TOP-GFP– or FOP-GFP (control)–transduced LME-1 cells treated with the porcupine inhibitors LGK974 or IWP-2 and stimulated with recombinant R-spondin 2. Error bars indicate ± SEM of three independent experiments in triplicate; ***P ≤ 0.001 using one-way ANOVA with Bonferroni correction.

R-spondins potentiate Wnt signaling in MM in a LGR4 dependent manner

Functionally, R-spondin binding to LGR4 facilitates Wnt pathway activation by stabilization of Wnt (co-)receptors, thereby increasing the sensitivity to Wnt ligands without activating Wnt signaling itself.[20,21] To establish whether the LGR4/R-spondin axis is instrumental in regulating Wnt signaling in MM cells, we initially assessed phosphorylation of the serine 1490 residue of LRP6 (Fig. S4A), which sequesters Axin to the plasma membrane[30], and the consequent stabilization and nuclear localization of β-catenin (Fig. 4A). As expected, stimulation with Wnt3a alone induced LRP6 phosphorylation and nuclear translocation of β-catenin in all MM cell lines tested (Fig 4A and S4A). However, stimulation with R-spondin alone did not result in Wnt pathway activation in the majority of cell lines (Fig 4A and S4A), but modestly increased Wnt signaling in LME-1 (3.1 fold increase in pLRP6 and 1.4 fold increase in nuclear β-catenin, Fig 4A and S4A), reflecting autocrine production of Wnts by the latter cells (see below). Simultaneous stimulation with R-spondin and Wnt ligands dramatically increased LRP6 phosphorylation and β-catenin stabilization/translocation in all LGR4-positive HMCLs tested, but not in the LGR4 negative cell line L363 (Fig 4A and S4A). To further study the role of LGR4 in amplification of Wnt signaling by R-spondin, we stably transduced HMCLs with a β-catenin sensitive fluorescent Wnt-reporter (TOP-GFP), which co-expresses a histone2B(H2B)/mCherry fusion protein as transduction-marker (Fig. S4B), combined with either inducible shRNA-mediated silencing (Fig. S4C) or CRISPR/Cas9-mediated gene disruption (Fig. 2D) of LGR4. FACS-sorted TOP-GFP⁺ MM cells displayed higher levels of nuclear β-catenin compared to TOP-GFP⁻ cells, confirming specificity of the reporter (Fig S4B). In line with the observed increase in LRP6 phosphorylation and β-catenin stabilization, R-spondin robustly amplified Wnt reporter activity in the presence of Wnt ligands (Fig 4B and S4C). Similar results were obtained upon transient transfection of the TOPflash luciferase reporter, which was activated up to 200-fold by simultaneous stimulation with Wnt3a and R-spondin (Fig. S5A). Importantly, shRNA-mediated silencing of LGR4 and CRISPR/Cas9-mediated LGR4 gene disruption abolished the potentiating effect of R-spondins on Wnt-pathway activation (Fig. 4B and Fig. S4C), indicating a crucial role for LGR4.

In LME1 cells, Wnt receptor stabilization by R-spondin increased Wnt pathway activity in the absence of exogenous Wnts (Fig. 4A/B S4A), suggesting autocrine Wnt production. Wnt secretion is dependent on palmitoylation by the porcupine enzyme, encoded by the *PORC* gene[31,32], and recently developed small molecule porcupine inhibitors (IWP-2, LGK974) efficiently block this Wnt secretion.[18,33,34] Both porcupine inhibitors strongly inhibited the robust stabilization of β-catenin and Wnt reporter activation observed upon stimulation of LME-1 with R-spondin alone (Fig. 4C and S5B), thus confirming the existence of an autocrine Wnt loop in.

2

Taken together, these results demonstrate that R-spondins facilitate auto- and paracrine Wnt signaling in MM in an LGR4-dependent manner and suggest that Wnt (co-) receptor levels are limiting in establishing high levels of Wnt-pathway activation in MM cells.

Inhibition of proximal Wnt/β-catenin signaling impairs proliferation in a subset of HMCLs

Downstream inhibition of Wnt/β-catenin signaling by a dominant negative form of TCF4 (dn.TCF4), shRNA mediated silencing of β-catenin, BCL9-like peptides or small molecule Wnt inhibitors has been previously shown to impair MM proliferation and expansion.[6,7,9,35] To confirm and extend these data, we expressed dnTCF4 in the HMCLs LME-1, RIES, and XG-1 from a bicistronic vector containing a fluorescent marker. Cells expressing dnTCF4 were rapidly outcompeted by cells that did not express dnTCF4 and incorporated less BrdU, confirming a role for Wnt signaling in MM cell expansion (Fig. 5A and S6A/B). Interestingly, in LME-1 and RIES inhibition of Wnt secretion by small molecule porcupine inhibitors also impaired growth (Fig. 5B), while XG-1 cells were unaffected (Fig. S6C), suggesting that the former two cell lines require autocrine Wnt secretion. Indeed, LME-1 cells displayed detectable levels of autocrine Wnt signaling (Fig 4 and S5B) while RIES cells were found to express extraordinary high levels of LGR4 (Fig S6D). As shown in figure 5C, doxycycline inducible, shRNA-mediated silencing of LGR4 (Fig. S6D) significantly impaired expansion of LME-1 and RIES (Fig. 5C), while silencing LGR4 in XG-1 had no apparent effect on cell growth (fig S6E). Taken together, these data indicate functional involvement of (autocrine) Wnts and the R-spondin/LGR4 axis in the growth of a subset of MMs.

R-spondins are produced in the BM niche by (pre)osteoblasts

Wnts have been shown to regulate hematopoietic stem cell (HSC) homeostasis and early B-cell development in a paracrine manner and their expression in the BM niche is well established.[36,37] However, the source of R-spondins remains to be defined. Prime candidates are osteoblasts, which have recently been suggested to utilize autocrine R-spondin for their differentiation[38] and, moreover, are a key constituents of the MM niche.[39,40] We therefore analyzed R-spondin mRNA expression in primary human osteoblasts (hOB) by qPCR. As expected, these cells expressed high levels of the osteoblastic markers *ALPL* (alkaline phosphatase), *BGLAP* (osteocalcin) and *COL1A1* (collagen 1A1), (Figure S7A). Interestingly, mRNA of all four R-spondins was readily detectable in primary hOB, with *RSPO2* and *RSPO3* showing the highest expression levels (Fig 6A). To extend these data and allow functional studies, we analyzed R-spondin expression in preosteoblast cell lines and *in vitro* differentiated osteoblasts, marked by high expression of the osteoblastic markers alkaline phosphatase (*akp2*) and osteocalcin (*bglap)* and high alkaline phosphatase (AP) activity. (Fig. S7B/C). *Rspo2* and *rspo3* mRNA was readily detectable in both preosteoblasts as well as

Fig. 5. Inhibition of Wnt signaling by suppression of β-catenin–mediated transcription, inhibition of Wnt secretion, or silencing of LGR4 impairs MM cell expansion.

(A) Percentage of MM cells transduced with control (black) or dnTCF4 (red), relative to t = 0, in a 7-d time course. Error bars indicate ± SEM of three independent transductions. *P ≤ 0.05, **P ≤ 0.01, and ***P ≤ 0.001 using unpaired Student's t-test. (B) Flow cytometry analysis of the effect of the small-molecule Wnt inhibitors IWP-2 and LGK974 on HMCL expansion after 4 d of culture, relative to day 0. Error bars indicate ± SEM of three independent transductions. *P ≤ 0.05 using unpaired Student's t-test. (C) Flow cytometry analysis of the effect of doxycycline-induced shRNA mediated silencing of LGR4 on MM cell expansion at day 4 of culture, relative to day 0. Error bars indicate ± SEM of three independent experiments in triplicate. *P ≤ 0.05 and **P ≤ 0.01 using unpaired Student's t-test.
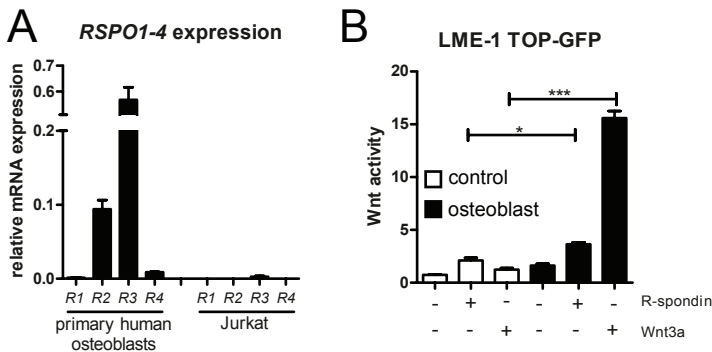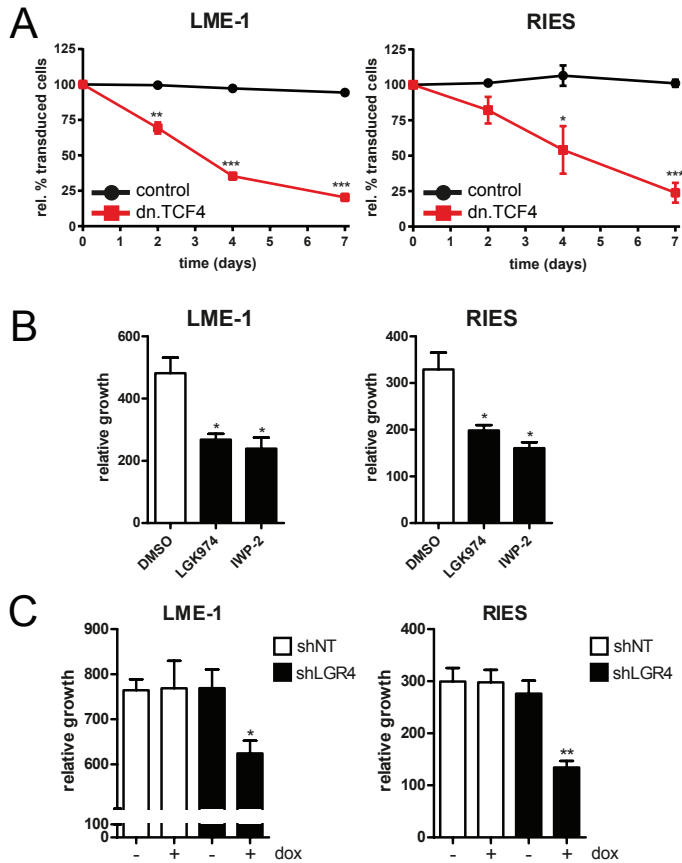

Fig. 6. (Pre)osteoblast-derived R-spondins facilitate auto- and paracrine Wnt signaling.
(A) qPCR analysis of RSPO1-4 mRNA levels in primary human osteoblasts from two independent donors. Jurkat cells served as a negative control. (B) Analysis of Wnt activity in TOP-GFP–transduced LME-1 cells treated with R-spondin 2 or low levels of Wnt3a (25 ng/mL) in the absence (white) or presence (black) of osteoblast-conditioned medium (KS483). Error bars indicate ± SEM of three independent experiments in triplicate; *P ≤ 0.05 and ***P ≤ 0.001 using one-way ANOVA with Bonferroni correction.

osteoblasts (Fig S7D). Surprisingly, R-spondin expression was markedly reduced in transition from preosteoblast to osteoblast. (Fig S7D). Functionally, (pre)osteoblast-conditioned media facilitated autocrine Wnt signaling in LME-1 and robustly synergized with exogenous Wnts in activating Wnt signaling in all cell lines tested (Fig 6B and S7E). However, by itself, and even if combined with exogenous R-spondins, they lack the capacity to activate Wnt signaling in OPM2 and XG-3 cells, indicating that functional Wnts are absent in (pre)osteoblast conditioned media. (Fig 6B and S7E). These results identify (pre)osteoblasts as a potential source of R-spondin in the BM niche that may facilitate Wnt/β-catenin signaling in MM via aberrantly expressed LGR4.

Discussion

Wnt/β-catenin pathway activation in MM is associated with disease progression and drug resistance, and mediates MM cell proliferation.[5-9] Since classical Wnt pathway activating mutations have not been described in MM, aberrant Wnt activity was proposed to be driven by the BM microenvironment. This Wnt pathway activation may be further boosted by epigenetic loss of Wnt pathway inhibitors, including sFRPs and DKK1[8,41,42] as well as by mutational inactivation of *CYLD*, a gene encoding a deubiquiting enzyme that negatively regulates Wnt signaling in MM[43], which are common events in advanced MM. However, the exact mechanism(s) driving Wnt pathway activation in MM remained undefined. Our current study demonstrates that Wnt pathway activation in MM is facilitated by a proximal event in the Wnt pathway, *i.e.* by aberrant expression of LGR4. This enables MM cells to hijack R-spondins produced by (pre)osteoblasts in the MM niche, thereby deregulating Wnt (co)receptor turnover and causing hypersensitivity of MM cells to autocrine and paracrine Wnts (Fig. S8).Interestingly, analysis of primary MM exome sequencing data from Lohr et al.[2] revealed that *RNF43* and *ZNRF3,* the E3-ligases that are subject to inhibition by LGR/ R-spondin signaling, harbor mutations in primary MM at low frequency (together 4/203, 2%). Mutations in these genes have been shown to drive Wnt signaling in other tumors[17-19], however, the effect of these specific mutations on Wnt signaling (in MM) remains to be established. In addition, analyzing the data of Mulligan et al.[44], involving targeted sequencing of established oncogenes, we identified a T41I mutation in β-catenin (*CTNNB1)* and a frameshift mutation in *APC* (S1465fs*3), both of which have been shown to drive oncogenic Wnt signaling.[45,46] Thus, these mutations might represent an alternative mechanisms driving Wnt signaling in a subset of MMs.

The seminal finding of our study is that LGR4 is expressed by the majority of pMMs and HMCLs, whereas normal bone marrow plasma cells and B cells are completely devoid of LGR4. This designates aberrant LGR4 expression as a hallmark of malignancy and suggests

that it can contribute to MM pathogenesis. Importantly, LGR4 expression is independent of the specific molecular MM subgroups, indicating that neither of the common MM subgroup-specific genomic alterations drives LGR4 expression. Rather, we found that STAT3 signaling, which is activated in the vast majority of MMs and is well known for its role in inflammation and cancer, mediates aberrant LGR4 expression.[26-28] This finding is of great interest since it links oncogenic Wnt activity in MM to inflammation and deregulated cytokine signaling. Although a wide variety of cytokines and growth factors are capable of activating STAT3, activation of STAT3 in MM typically results from auto- or paracrine IL-6 signaling.[26,28] Indeed, we found that IL-6 stimulation leads to STAT3-mediated LGR4 upregulation. Recently, Dechow et al.[27] reported that chronic STAT3 activation cooperates with MYC, which is a transcriptional target of β-catenin[16], in the development of MM. This underscores the importance of simultaneous activation of STAT3 signaling and Wnt/β-catenin signaling in MM pathogenesis.

Wnts are produced by BM stromal cells and play a role in the control of hematopoietic stem cell homeostasis and early B-cell development.[36,37] Likewise, Wnt signaling in MM can be activated by paracrine Wnt ligands emanating from the BM niche, which is mimicked *in vitro* by stimulation with exogenous Wnts. In addition, gene-expression studies showed overexpression of Wnts in MM[6,8], suggesting autocrine signaling. Our functional studies show that R-spondin/LGR4 interaction strongly amplifies the response to exogeneous/paracrine Wnts. Moreover, the finding that R-spondin can also potentiate Wnt signaling in the absence of exogenously added Wnts, and that small molecule inhibitors of Wnt secretion mitigates this effect, firmly establishes the existence of an autocrine Wnt-signaling loop in a subset of MMs. Downstream inhibition of Wnt signaling was previously shown to impair MM proliferation[5-7,9,35]. Interestingly, our current results indicate that a subset of HMCLs are also sensitive to proximal Wnt pathway inhibition by porcupine inhibitors and LGR4 silencing. MM cell lines are almost invariably derived from MM cells in a leukemic phase of the disease at which the malignant cells have lost their dependence upon the BM niche. By contrast, however, the vast majority of primary MMs is strictly dependent upon a protective BM niche for growth and survival. Therefore, primary MM will most likely be more vulnerable to inhibition of Wnts and/or R-spondins emanating from the BM niche.

Whereas the presence of Wnt ligands in the BM niche is well established, expression of R-spondins in the BM microenvironment thus far has remained largely unexplored. Since autocrine R-spondins have been suggested to regulate differentiation of osteoblast[38], which are important constituents of the MM niche[39,40], we hypothesized that osteoblasts could be a major source of R-spondins driving oncogenic Wnt signaling. Corroborating this hypothesis, we found expression of several R-spondins in (pre)osteoblasts and demonstrated that (pre)osteoblast conditioned media robustly synergized with Wnt ligands in activating Wnt signaling. Notably, we observed that R-spondin expression decreases during differentiation

2

of preosteoblasts to osteoblasts. This suggests a scenario in which active suppression of osteoblast differentiation by MM cells[47] may lead to increased local levels of R-spondins, creating a feed-forward loop that drives Wnt-signaling in the tumor cells.

In summary, we have uncovered a previously unknown role for the LGR4/R-spondin axis in regulating Wnt/β-catenin in MM cells. Importantly, we demonstrate that the R-spondin effects are fully dependent on LGR4, implying that, unlike in intestinal epithelium where LGR4 and LGR5 have redundant functions, therapeutic targeting of LGR4 in MM will be sufficient to abolish R-spondin-mediated Wnt signaling amplification. These findings identify LGR4/R-spondin signaling as a novel therapeutic target for MM patients.

Materials and Methods

For additional information on methods, see SI Materials and Methods.

Plasmids and Cloning

pTRIPZ-shLGR4 and pTRIPZ-shSTAT3 were constructed as previously described.[48] In short, a 97-mer template was amplified by PCR and inserted in the XhoI/EcoRI site of the pTRIPZ vector (Thermo Scientific, Waltham, MA). Targeting sequences were GCGTAATCAAATCTACCAAAT (hLGR4) and GCACAATCTACGAAGAATCAA (hSTAT3). pLentiCrispr-sgLGR4 was constructed by inserting sgLGR4 (GCAGCTGCGACGGCGACCGT, chr11:27493733-27493752, hg19) in pLentiCrispr (Addgene, Cambridge, MA, 52961) as previously described.[49] TOP-GFP.mCh/FOP-GFP.mCh (Addgene 35491 and 35492) were kind gifts from David Horst.[50] pEF.STAT3DN.Ubc.GFP (24984), pEF.STAT3C.Ubc.GFP (24983) and EdTC (dnTCF4, 24310) were obtained from Addgene.

Micro-array data analysis

Datasets presented in figure 1 and figure S1A/B were obtained from the publically available Amazonia! web atlas[51] and normalized by global scaling to 100 and include samples representing naïve B cells (n=5), centroblasts (n=4), centrocytes (n=4), memory B cells (n=5), plasmablasts (n=5), bone marrow plasma cells (n=5)[52], CD4+ T cells (n=4), CD8+ T cells (n=6)[53], chronic myeloid leukemia (n=35)[54], acute myeloid leukemia (n=89)[55,56], B cell acute lymphoblastic leukemia (n=82)[57] (Lugo-Trampe et al. GSE10820), T cell acute lymphoblastic leukemia (n=54) (Winter et al. GSE14615), diffuse large B cell lymphoma (n=51)[58], follicular lymphoma (n=20)[59], chronic lymphoid leukemia (n=124) [54,60-62], multiple myeloma (n=30) and intestinal tissues (n=8) (Roth et al. GSE7307). The micro-array dataset presented in figure S1C and figure S1D contained gene-expression data of primary MM samples divided in subgroups based on molecular profiling that was normalized as described.[25] Molecular subgroups were previously identified and include the CD1 (n=18), CD2 (n=26), hyperdyploïd (n=47), low bone disease (n=23), MAF/MAFB (n=13), MMSET (n=36), myeloid gene signature (n=71) and proliferation (n=21) subgroups.

Acknowledgments

Authorship

H.vA. designed the research, performed most in vitro experiments, analyzed the data, designed the figures and wrote the paper; I.K. provided technical assistance. Z.R. and S.P.J. performed in vitro experiments and reviewed the manuscript. K.A.K., A.M.d.B and J.E.J.G. helped design the research and reviewed the manuscript. W.dL. and H.C. developed LGR4-specific mAbs and reviewed the manuscript. M.S. and S.T.P. supervised the study, designed the research and analyzed the data and STP wrote the paper.

2

Reference list

1. Morgan GJ, Walker BA, Davies FE. (2012) The genetic architecture of multiple myeloma. *Nat Rev Cancer* 12:335-348.

2. Lohr JG, et al. (2014) Widespread genetic heterogeneity in multiple myeloma: implications for targeted therapy. *Cancer Cell* 25(1):91-101.

3. Lawasut P, et al. (2013) Decoding the pathophysiology and the genetics of multiple myeloma to identify new therapeutic targets. *Semin Oncol* 40:537-48.

4. Hideshima T, Mitsiades C, Tonon G, Richardson PG, Anderson KC. (2007) Understanding multiple myeloma pathogenesis in the bone marrow to identify new therapeutic targets. *Nat Rev Cancer* 7:585-98.

5. Ashihara E, et al. (2009) Beta-catenin small interfering RNA successfully suppressed progression of multiple myeloma in a mouse model. *Clin Cancer Res* 15:2731-2738.

6. Derksen PW, et al. (2004) Illegitimate WNT signaling promotes proliferation of multiple myeloma cells. *Proc Natl Acad Sci USA* 101:6122-6127.

7. Dutta-Simmons J, et al. (2009) Aurora kinase A is a target of Wnt/beta-catenin involved in multiple myeloma disease progression. *Blood* 114:2699-2708.

8. Kocemba KA, et al. (2012) Transcriptional silencing of the Wnt-antagonist DKK1 by promoter methylation is associated with enhanced Wnt signaling in advanced multiple myeloma. *PLoS One* 7:e30359.

9. Sukhdeo K, et al. (2007) Targeting the beta-catenin/TCF transcriptional complex in the treatment of multiple myeloma. *Proc Natl Acad Sci USA* 104:7516-7521.

10. Clevers H, Nusse R. (2012) Wnt/beta-catenin signaling and disease. *Cell* 149:1192-1205.

11. Clevers H, Loh KM, Nusse R. (2014) Stem cell signaling. An integral program for tissue renewal and regeneration: Wnt signaling and stem cell control. *Science* 346:1248012.

12. Behrens J, et al. (1996) Functional interaction of beta-catenin with the transcription factor LEF-1. *Nature* 382: 638-642.

13. Molenaar M, et al. (1996) XTcf-3 transcription factor mediates beta-catenin-induced axis formation in Xenopus embryos. *Cell* 86:391-399.

14. He TC, et al. (1998) Identification of c-MYC as a target of the APC pathway. *Science* 281:1509-1512.

15. Tetsu O, McCormick F. (1999) Beta-catenin regulates expression of cyclin D1 in colon carcinoma cells. *Nature* 398:422-426.

16. Tagde A, et al. (2016) MUC1-C drives MYC in multiple myeloma. *Blood* 65915 Epub

17. de Lau W, Peng WC, Gros P, Clevers H. (2014) The R-spondin/Lgr5/Rnf43 module: regulator of Wnt signal strength. *Genes Dev* 28:305-16.

18. Jiang X, et al. (2013) Inactivating mutations of RNF43 confer Wnt dependency in pancreatic ductal adenocarcinoma. *Proc Natl Acad Sci USA* 110:12649-12654.

19. Wu J, et al. (2011) Whole-exome sequencing of neoplastic cysts of the pancreas reveals recurrent

mutations in components of ubiquitin-dependent pathways. *Proc Natl Acad Sci USA* 108:21188-21193.

20. de Lau W, et al. (2011) Lgr5 homologues associate with Wnt receptors and mediate R-spondin signalling. *Nature* 476:293-297.

21. Carmon KS, Gong X, Lin Q, Thomas A, Liu Q. (2011) R-spondins function as ligands of the orphan receptors LGR4 and LGR5 to regulate Wnt/beta-catenin signaling. *Proc Natl Acad Sci USA* 108:11452-11457.

22. Hao HX, et al. (2012) ZNRF3 promotes Wnt receptor turnover in an R-spondin-sensitive manner. *Nature* 485:195-200.

23. Koo BK, et al. (2012) Tumour suppressor RNF43 is a stem-cell E3 ligase that induces endocytosis of Wnt receptors. *Nature* 488:665-669.

24. Sato T, et al. (2009) Single Lgr5 stem cells build crypt-villus structures in vitro without a mesenchymal niche. *Nature* 459:262-265.

25. Zhan F, et al. (2006) The molecular classification of multiple myeloma. *Blood* 108:2020-2028.

26. Catlett-Falcone R, et al. (1999) Constitutive activation of Stat3 signaling confers resistance to apoptosis in human U266 myeloma cells. *Immunity* 10:105-115.

27. Dechow T, et al. (2014) GP130 activation induces myeloma and collaborates with MYC. *J Clin Invest* 124:5263-5274.

28. Kawano M, et al. (1988) Autocrine generation and requirement of BSF-2/IL-6 for human multiple myelomas. *Nature* 332:83-85.

29. Liu J, et al. (2013) Stat3 upregulates leucine-rich repeat-containing g protein-coupled receptor 4 expression in osteosarcoma cells. *Biomed Res Int* 310691.

30. Niehrs C. (2012) The complex world of WNT receptor signalling. *Nat Rev Mol Cell Biol* 12:767-79.

31. Willert K, et al. (2003) Wnt proteins are lipid-modified and can act as stem cell growth factors. *Nature* 423:448-452.

32. Kadowaki T, Wilder E, Klingensmith J, Zachary K, Perrimon N. (1996) The segment polarity gene porcupine encodes a putative multitransmembrane protein involved in Wingless processing. *Genes Dev* 10:3116-3128.

33. Chen B, et al. (2009) Small molecule-mediated disruption of Wnt-dependent signaling in tissue regeneration and cancer. *Nat Chem Biol* 5:100-107.

34. Liu J, et al. (2013) Targeting Wnt-driven cancer through the inhibition of Porcupine by LGK974. *Proc Natl Acad Sci USA* 110:20224-20229.

35. Takada T, et al. (2012) Targeted disruption of the BCL9/β-catenin complex inhibits oncogenic Wnt signaling. *Sci Transl Med* 148:148ra117.

36. Reya T, et al. (2000) Wnt signaling regulates B lymphocyte proliferation through a LEF-1 dependent mechanism. *Immunity* 13:15-24.

37. Reya T, et al. (2003) A role for Wnt signalling in self-renewal of haematopoietic stem cells. *Nature* 423:409-414.

2

38. Friedman MS, Oyserman SM, Hankenson KD. (2009) Wnt11 promotes osteoblast maturation and mineralization through R-spondin 2. *J Biol Chem* 284:14117-14125.

39. Toscani D, Bolzoni M, Accardi F, Aversa F, Giuliani N. (2015) The osteoblastic niche in the context of multiple myeloma. *Ann NY Acad Sci* 1335:45-62.

40. Chen Z, Orlowski RZ, Wang M, Kwak L, McCarty N. (2014) Osteoblastic niche supports the growth of quiescent multiple myeloma cells. *Blood* 123:2204-2208.

41. Chim CS, Pang R, Fung TK, Choi CL, Liang R. (2007) Epigenetic dysregulation of Wnt signaling pathway in multiple myeloma. *Leukemia* 21:2527-2536.

42. Jost E, et al. (2009) Epigenetic dysregulation of secreted Frizzled-related proteins in multiple myeloma. *Cancer Lett* 281:24-31.

43. Van Andel H, et al. (2016) Loss of CYLD expression unleashes Wnt signaling in multiple myeloma and is associated with aggressive disease. *Oncogene* in press.

44. Mulligan G, et al. (2014) Mutation of NRAS but not KRAS significantly reduces myeloma sensitivity to single-agent bortezomib therapy. *Blood* 123:632-639.

45. Van Noort M, (2002) Identification of two novel regulated serines in the N terminus of beta-catenin. *Exp Cell Res* 276:264-72.

46. Martin-Denavit T, (2001) Phenotype variability of two FAP families with an identical APC germline mutation at codon 1465: a potential modifier effect? *Clin Genet.* 60:125-131

47. Tian E, et al. (2003) The role of the Wnt-signaling antagonist DKK1 in the development of osteolytic lesions in multiple myeloma. *N Engl J Med* 349:2483-2494.

48. Dow LE, et al. (2012) A pipeline for the generation of shRNA transgenic mice. *Nat Protoc* 7:374-393.

49. Sanjana NE, Shalem O, Zhang F. (2014) Improved vectors and genome-wide libraries for CRISPR screening. *Nat Methods* 11:783-784.

50. Horst D, et al. (2012) Differential WNT activity in colorectal cancer confers limited tumorigenic potential and is regulated by MAPK signaling. *Cancer Res* 72:1547-1556.

51. Le Carrour T, et al. (2010) Amazonia!: An Online Resource to Google and Visualize Public Human whole Genome Expression Data. *The Open Bioinformatics Journal* 4:5-10.

52. Jourdan M, et al. (2009) An in vitro model of differentiation of memory B cells into plasmablasts and plasma cells including detailed phenotypic and molecular characterization. *Blood* 114:5173-81.

53. Piccaluga PP, et al. (2007) Gene expression analysis of peripheral T cell lymphoma, unspecified, reveals distinct profiles and new potential therapeutic targets. *J Clin Invest* 117:823-34.

54. Haferlach T, et al. (2010) Clinical utility of microarray-based gene expression profiling in the diagnosis and subclassification of leukemia: report from the International Microarray Innovations in Leukemia Study Group. *J Clin Oncol* 28:2529-37.

55. Verhaak RG, et al. (2009) Prediction of molecular subtypes in acute myeloid leukemia based on gene expression profiling. *Haematologica* 94:131-4.

56. Payton JE, et al. (2009) High throughput digital quantification of mRNA abundance in primary human acute myeloid leukemia samples. *J Clin Invest* 119:1714-26.

57. Bungaro S, et al. (2009) Integration of genomic and gene expression data of childhood ALL without known aberrations identifies subgroups with specific genetic hallmarks. *Genes Chromosomes Cancer* 48:22-38.

58. Lenz G, et al. (2008) Stromal gene signatures in large-B-cell lymphomas. *N Engl J Med* 359:2313-23.

59. Compagno M, et al. (2009) Mutations of multiple genes cause deregulation of NF-kappaB in diffuse large B-cell lymphoma. *Nature* 459:717-21.

60. Ouillette P, et al. (2008) Integrated genomic profiling of chronic lymphocytic leukemia identifies subtypes of deletion 13q14. *Cancer Res* 68:1012-21.

61. Giannopoulos K, et al. (2009) Thalidomide exerts distinct molecular antileukemic effects and combined thalidomide/fludarabine therapy is clinically effective in high-risk chronic lymphocytic leukemia. *Leukemia* 23:1771-8.

62. Friedman DR, et al. (2009) A genomic approach to improve prognosis and predict therapeutic response in chronic lymphocytic leukemia. *Clin Cancer Res* 15:6947-55.

2

Supporting Materials and Methods

Cell culture and treatment

The human multiple myeloma cell lines (HMCLs) ANBL-6, L363, LME-1, NCI-H929, OPM-2, RPMI 8226, U266, UM-3, XG-1, RIES and XG-3 were cultured in IMDM medium (Invitrogen Life Technologies, Carsbad, CA) containing 10% FBS (Invitrogen Life Technologies), 100 units/ml penicillin (Sigma Aldrich, St. Louis, MO), 100 µg/ml streptomycin (Sigma Aldrich), 20 µg/ml human apo-transferrin (Sigma Aldrich) and 50 µM β-mercaptoethanol (Sigma Aldrich). For XG-1, XG-3, ANBL-6, RIES and LME-1 medium was supplemented with 500 pg/mL IL-6 (Prospec, East Brunswick, NJ). For growth assays, pTRIPZshRNA transduced HMCLs were incubated for 96h with doxycycline to establish knockdown. Cells were seeded at 15000 cells per well in a 96-well plate in culture medium containing 2% FCS. Dead cells (TO-PRO-3-Iodide$^+$) were excluded for analysis. Murine KS483 cells, MC3T3-E1 subclone 4 cells (ATCC CRL-5293) and C3H10t1/2 clone 8 (ATCC CLL-226) cells were maintained in MEM-α medium (Invitrogen) supplemented with 10% FBS (Invitrogen), 100 units/ml penicillin, and 100 µg/ml streptomycin. Osteoblast differentiation was induced by 96h treatment of preosteoblast cells with 50 µg/ml ascorbic acid, 10 nM dexamethasone and 100ng/mL hBMP4/7 heterodimers (R&D systems, Minneapolis, MN). For alkaline phosphatase (AP) substrate staining cells were fixed in 10% formalin, permeabilized with 0,05% tween/TBS and stained with NBT/BCIP (Roche, Basel, Switzerland) according to the manufacturer's instructions. Lysates of primary human osteoblasts were obtained from PromoCell (Heidelberg, Germany).

For signal transduction experiments, recombinant hWnt3a (R&D systems) was used at 100ng/mL, recombinant hR-spondin 2 at 50ng/mL (R&D systems) and hIL-6 (Prospec) at 50ng/mL unless otherwise stated. Wnt inhibitors used were IWP-2 (2.5uM, Stemgent, Lexington, MA) and LGK974 (2uM, StemRD, Burlingame, CA).

Transfection and Transduction

Lentiviral particles were produced by transfecting HEK293T cells with pMD2.G/VSVG (12259), pPAX2 (12260) and the lentiviral vector in a 6:15:20 ratio with Genius™ DNA transfection reagent (Westburg, Leusden, The Netherlands) according to the manufacturer's instructions. MM cells were spinfected for 60 minutes with 1800RPM at 33°C in the presence of 8ug/mL polybrene (Sigma Aldrich). 72 hour after transduction, cells were FACS-sorted or selected with puromycin (Sigma Aldrich). For transient luciferase reporter experiments, 10×10^6 cells were electroporated with the TOPflash/FOPflash Wnt reporter (10 µg) and pRL-TK-Renilla (2 µg). After 24h of recovery, cells were stimulated overnight. Luciferase activity was measured using the dual luciferase assay kit (Promega, Madison, WI) using a GloMax-Multi+ (Promega) according to the manufacturer's instructions.

qRT-PCR

Total RNA was isolated using TRIreagent (Invitrogen Life Technologies) according to the manufacturer's instructions and converted to cDNA using oligo-dT. PCRs were conducted using SensiFast (Bioline, London, UK) on a CFX384 RT-PCR detection system (Biorad, Hercules, CA). Primer sequences are shown in table S1.

Immunoblotting

Protein samples (whole-cell extracts in radio-immunoprecipitation assay lysis buffer (RIPA)) were separated by 10% SDS-polyacrylamide gel electrophoresis and subsequently blotted. Nuclear and cytosolic fractions were prepared using the Nuclear/Cytosolic fractionation kit (Biovision, Milpitas, CA) according to the manufacturer's instructions. The antibodies used were: mouse anti-β-tubulin (clone D66, Sigma Aldrich), mouse anti-β-actin (clone AC-15, Sigma Aldrich), mouse anti-β-catenin (clone 14, BD Biosciences, Franklin Lakes, NJ), mouse anti-LRP6 (clone C47E12, Cell Signaling, Danvers, MA), polyclonal rabbit anti-pLRP6 (Cell Signaling), mouse anti-STAT3 (clone 124H6, Cell Signaling), polyclonal rabbit anti-pSTAT3 (Tyr705, Cell Signaling) and polyclonal rabbit anti-Lamin A/C (Santa Cruz, Dallas, TX). Primary antibodies were detected by HRP-conjugated secondary antibodies (DAKO, Glostrup, Denmark), followed by detection using Amersham ECL Westernblot Detection Reagent (GE Healthcare, Little Chalfont, UK). Quantification of immunoblots was done using Image J software.

Flow cytometry

For LGR4 and LGR5 (clone 4D11) staining, cells were incubated with hybridoma supernatants containing hLGR4 specific rat monoclonal IgG2b antibodies, followed by staining with biotinylated mouse-anti-rat IgG2b (clone MRG2b-85, Biolegend, San Diego, CA) and streptavidin-APC (Southern Biotech, Birmingham, AL). For Phosflow intracellular stainings, cells were stained with anti-pSTAT3-PE (clone 4/pSTAT3, BD Biosciences) or isotype control antibodies (clone MOPC-173, BD Biosciences) using the Cytofix/Cytoperm kit (BD Biosciences) according to the manufacturer's instructions. Human tonsillar mononuclear cells were isolated by Ficoll-Paque (GE Healthcare) gradient centrifugation, followed by staining with CD19-APC.H7 (clone SJ25C1), CD38-APC (clone HIT2), CD27-FITC (clone M-T271) and IgD-V450 (all from BD Biosciences). For isolation of primary MM cells, mononuclear cells were isolated from fresh BM aspirates using Ficoll-Paque (GE-Healthcare) gradient centrifugation, followed by MACS-separation using anti-CD138 microbeads (Clone B-B4, Milteny, Leiden, the Netherlands). For cell cycle analysis, cells were incubated for 0.5 – 1h with 20μM BrdU (Sigma Aldrich) and subsequently fixed in ice-cold 70% ethanol. After washing, cells were incubated in 0.4mg/mL pepsin/0.2mM HCl for 30' on RT and subsequently in 2M HCl for 25' at 37°C. Cells were washed with 0,05%Tween-20/0,5%BSA in PBS (PBS-TB) and stained for 30' with anti-BrdU FITC (clone B44, BD Biosciences) in PBS-TB.

2

After washing, cells were treated with 500µg/mL RNAse-A (Bioke, Leiden, The Netherlands) and stained with 0,1µM TO-PRO-3-Iodide (Invitrogen Life Technologies) for 15' at 37°C.
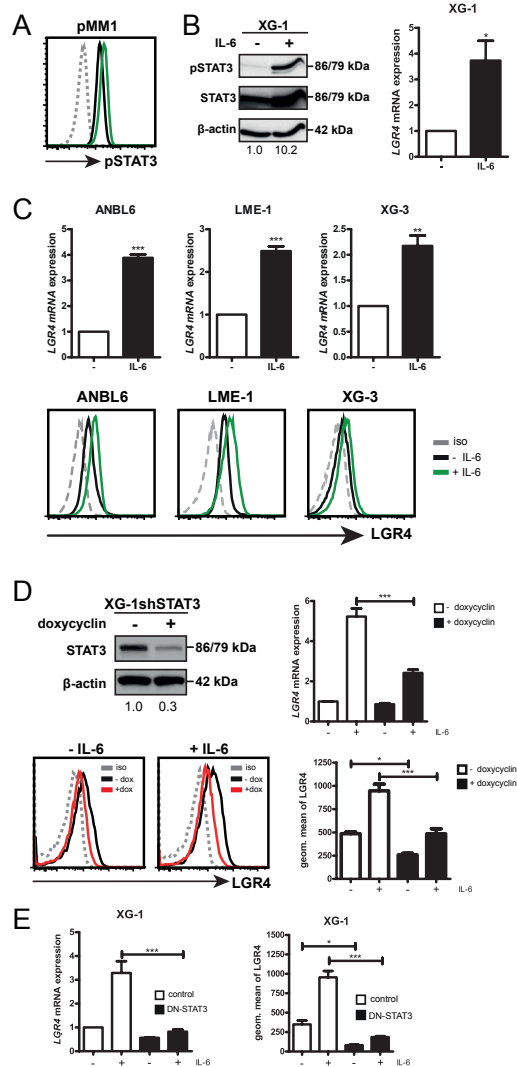
Supplementary data
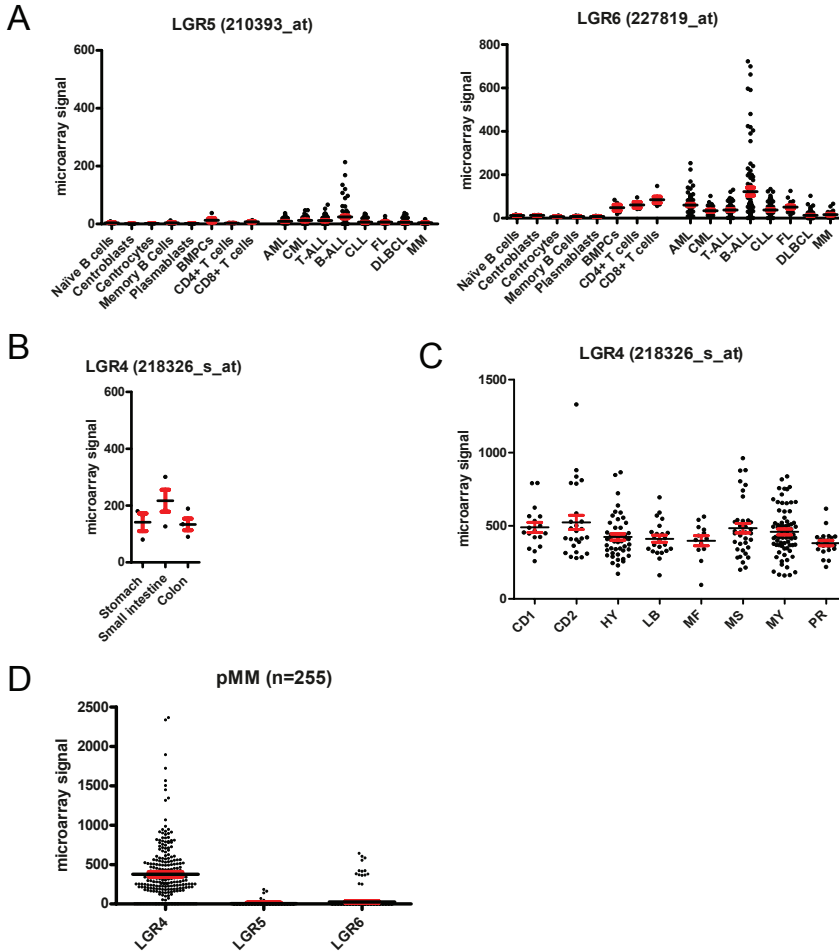
Supplementary figure 1. (A) Analysis of LGR5 (left panel) and LGR6 (right panel) mRNA expression in publically available microarray datasets. BMPC=bone marrow plasma cells, CML=chronic myeloid leukemia, AML=acute myeloid leukemia, B-ALL=B-cell acute lymphoblastic leukemia, T-ALL=T-cell acute lymphoblastic leukemia, DLBCL=diffuse large B cell lymphoma, FL=follicular lymphoma, CLL=chronic lymphoid leukemia. Data was normalized by global scaling to 100. ***, P ≤ 0.001 using one-way ANOVA with Bonferroni correction. (B) Analysis of LGR4 mRNA expression in a publically available microarray dataset containing samples representing stomach, small intestinal and colon tissue. Data was normalized by global scaling to 100. (C) LGR4 mRNA expression in MM samples divided in subgroups based on molecular profiling. HY=hyperdyploïd, LB=low bone disease, MF=MAF/MAFB, MS=MMSET, MY=myeloid gene signature, PR=proliferation subgroup. Data was normalized by Zhan et al.[25] (D) Analysis of LGR4, LGR5 and LGR6 expression in a microarray dataset containing 255 pMMs.
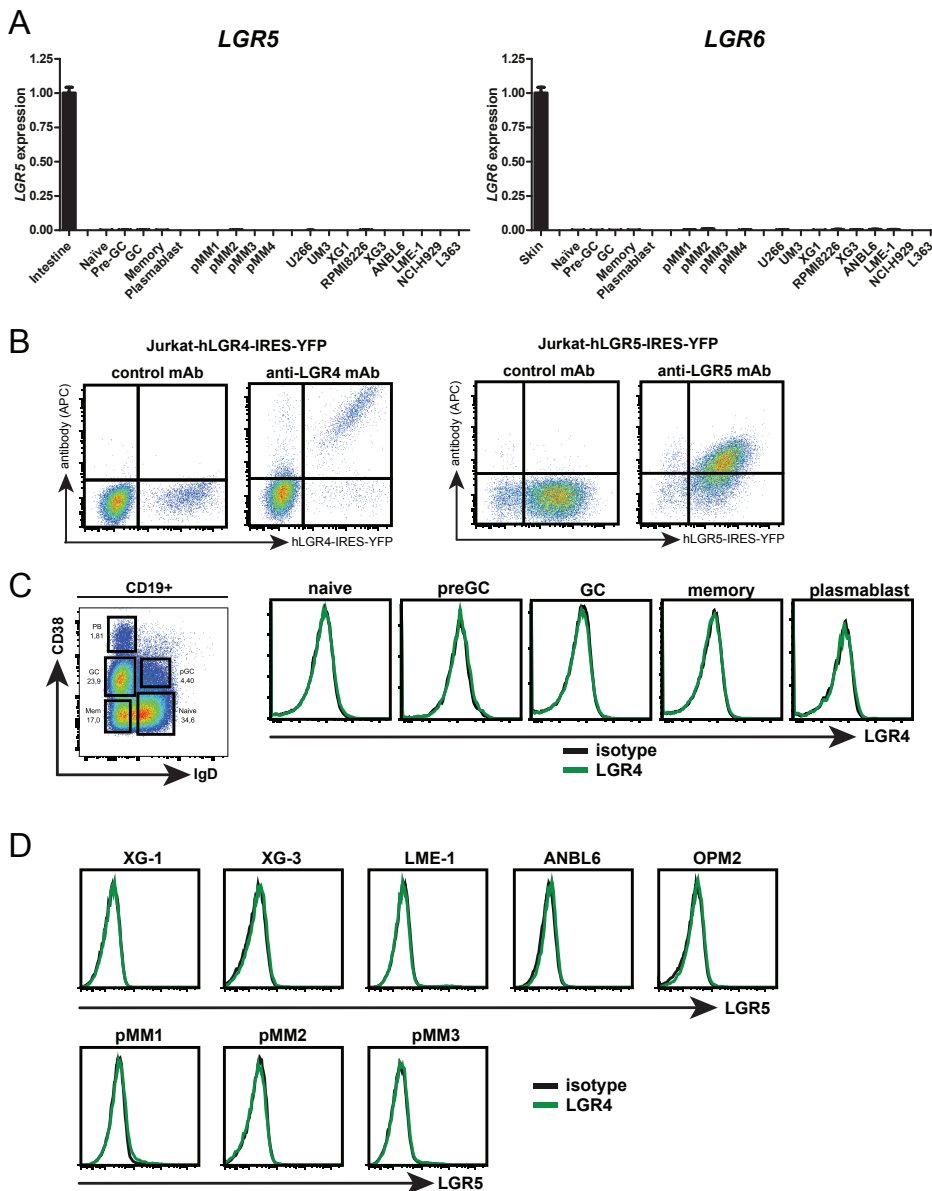
Supplementary figure 2. (A) LGR5 (left) and LGR6 (right) mRNA expression in normal B-cell subsets (n=5), pMMs (n=4), and HMCLs (n=9), analyzed by qPCR and normalized to TBP. Expression levels were compared to normal intestinal tissue for LGR5 and normal skin tissue for LGR6. (B) Flow cytometry analysis of Jurkat cells (LGR4 and LGR5 negative) transduced with full length human LGR4 (left) or LGR5 (right) from a bicistronic vector containing YFP, stained with a control mAb, LGR4 specific mAb or LGR5 specific mAb. (C) LGR4 protein expression in B cells subsets defined by staining with CD19, CD38 and IgD. (D) Flow cytometry analysis of LGR5 expression in HMCLs (n=5) and pMMs (n=3).

2

Supplementary figure 3. (A) Flow cytometry analysis of pSTAT3 (Tyr705) in pMM1 stimulated with IL-6. (B) Western blot for pSTAT3 (Tyr705), total STAT3 and β-actin in XG-1 cells treated with or without IL-6 for 24h, representative for 3 independent experiments (left). Densitometric quantification (pSTAT3/β-actin) relative to unstimulated conditions is shown below. qPCR for LGR4 mRNA normalized to TBP in XG-1 cells treated with or without IL-6 (right). (C) qPCR for LGR4 mRNA normalized to TBP (top) and flow cytometry analysis of LGR4 (bottom) in three HMCLs treated with or without IL-6 for 24h. Error bars indicate ±SEM of 3 independent experiments **, P ≤ 0.01; ***, P ≤ 0.001 using un-paired student's t test. (D) Western blot for STAT3 after doxycycline-induced shRNA-mediated STAT3 silencing in XG-1 cells, representative for 3 independent experiments. β-actin was used as a loading control (top left). Densitometric quantification (STAT3/β-actin) relative to unstimulated conditions is shown below. qPCR analysis of LGR4 mRNA normalized to TBP (top right) and flow cytometry analysis (bottom left) with quantification of geometric mean (bottom right) of LGR4 expression in XG-1 after induction of shSTAT3 and treatment with IL-6. Error bars indicate ±SEM of 3 independent experiments in triplicate *, P ≤ 0.05, ***, P ≤ 0.001 using one-way ANOVA with Bonferroni correction. (E) qPCR analysis of LGR4 mRNA expression (left) and quantification of geometric mean of flow cytometry analysis of LGR4 (right) in control or DN.STAT3 transduced XG-1 cells treated with IL-6 for 24h. Error bars indicate ±SEM of 3 independent experiments in triplicate *, P ≤ 0.05, ***, P ≤ 0.001 using one-way ANOVA with Bonferroni correction.
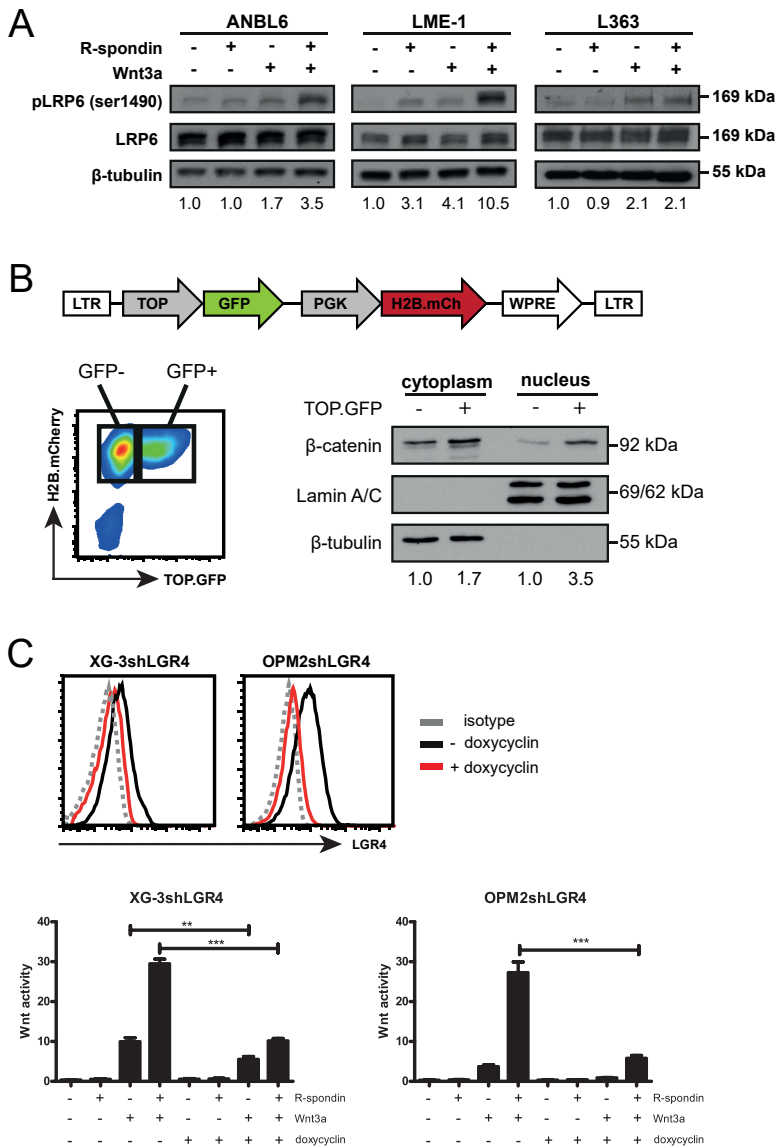
Supplementary figure 4. (A) Western blot analysis of pLRP6, LRP6 and β-tubulin in LGR4^{hi} (ANBL6 and LME-1) and LGR4^{lo} (L363) HMCLs treated with recombinant R-spondin 2, Wnt3a or both, representative for 5 independent experiments. Densitometric quantification (pLRP6/LRP6) relative to unstimulated conditions is shown below. (B) Schematic representation of the lentiviral TOP.GFP/H2B.mCherry Wnt reporter plasmid (top). Analysis of subcellular distribution of β-catenin in FACS sorted TOP-GFP$^-$ or TOP-GFP$^+$ OPM-2 cells treated with recombinant Wnt3a and R-spondin 2 by western blot, representative for 3 independent experiments (bottom). β-tubulin (cytoplasm) and lamin A/C (nucleus) served as a fractionation and loading control. Densitometric quantification (β-catenin/lamin A/C for nuclear fractions and β-catenin/β-tubulin for cytoplasmic fractions) relative to unstimulated conditions is shown below. (C) Flow cytometry analysis of LGR4 protein expression in HMCLs with (black) or without (red) doxycycline-induced shRNA-mediated LGR4 knockdown (top). Flow cytometry analysis of Wnt activity in TOP. GFP transduced HMCLs treated with R-spondin 2, Wnt3a or both after shRNA mediated LGR4 silencing (bottom).

A   **LGR4 positive**   **LGR4 negative**

2

B
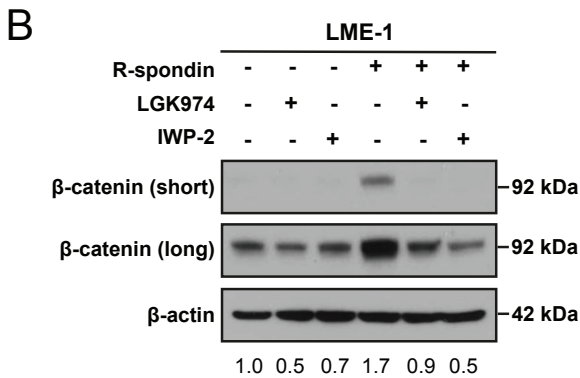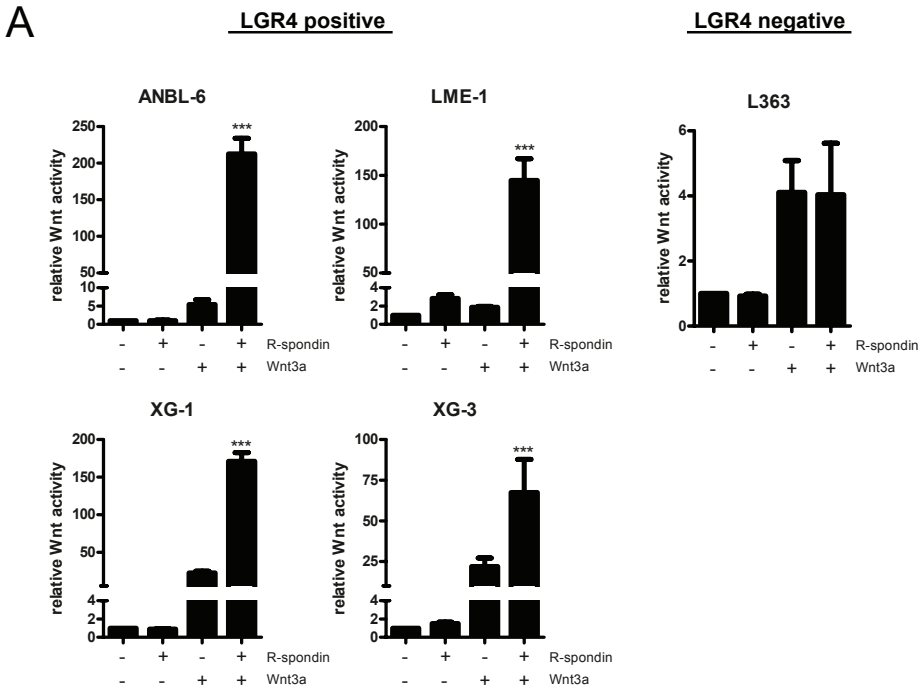
Supplementary figure 5. (A) Analysis of Wnt activity in MM cells stimulated with recombinant Wnt3a and/or R-spondin by transfection of the Top-luciferase Wnt reporter. Top-luciferase values were normalized to TK-Renilla luciferase activity (RLU) and values were plotted as relative to unstimulated conditions. Error bars indicate ±SEM of 3 independent experiments in triplicate ***, P ≤ 0.001 using one-way ANOVA with Bonferroni correction. (B) Western blot analysis of β-catenin stabilization in LME-1 cells treated with porcupine inhibitors LGK974 or IWP-2 and stimulated with recombinant R-spondin 2, representative for 3 independent experiments. β-actin was used as a loading control. Densitometric quantification (β-catenin/β-actin) relative to unstimulated conditions is shown below.
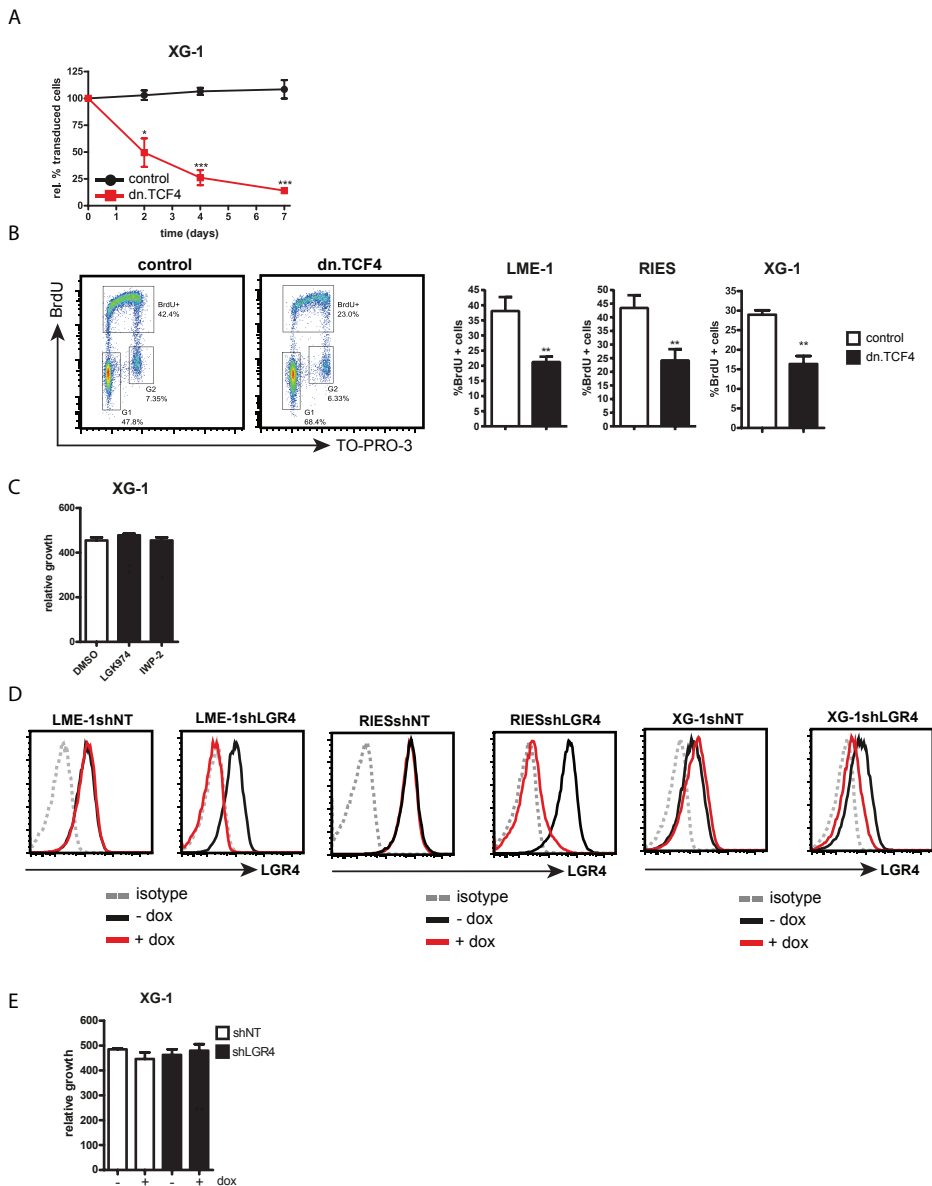
Supplementary figure 6. (A) Percentage of XG-1 cells transduced with control (black) or dn.TCF4 (red) relative to t=0, in a 7 day time course. Error bars indicate ±SEM of 3 independent transductions. *, P ≤ 0.05, ***, P ≤ 0.001 using unpaired student's t test. (B) Representative picture of cell cycle analyses after BrdU incorporation in control or DN.TCF4 transduced, sorted LME-1 cells (left) and quantification of BrdU incorporation in three HMCLs (right). Error bars indicate ±SEM of 3 independent transductions. **, P ≤ 0.01 using unpaired student's t test. (C) Flow cytometry analysis of the effect of the small molecule Wnt inhibitors IWP-2 and LGK974 on expansion of XG-1 cells after 4 days of culture, relative to day 0. (D) Flow cytometry analysis of LGR4 expression in HMCLs transduced with doxycycline-inducible non-targeting or LGR4 targeting shRNAs treated with (red) or without (black) doxycylin. (E) Flow cytometry analysis of the effect of doxycycline-induced shRNA-mediated silencing of LGR4 on expansion of XG-1 cells at day 4 of culture, relative to day 0.
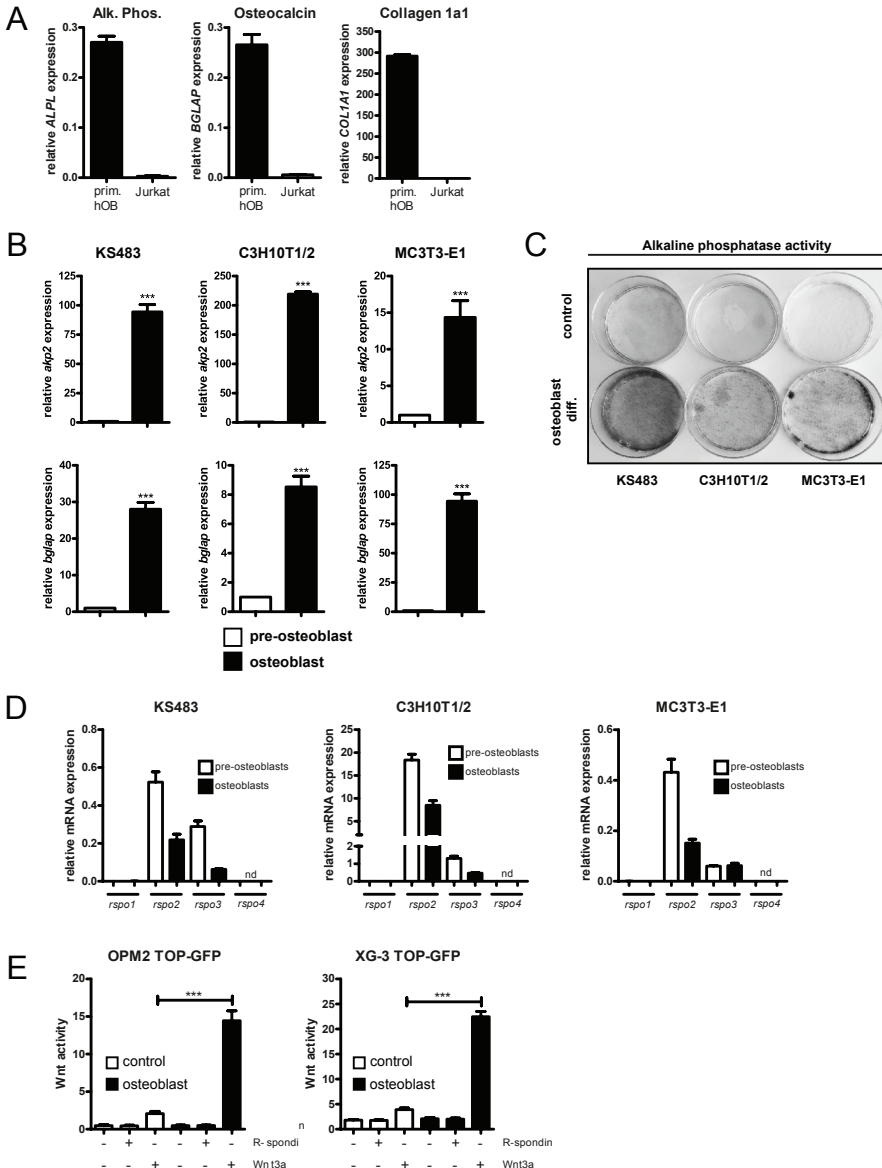
Supplementary figure 7. (A) qPCR analysis of alkaline phosphatase (ALPL), osteocalcin (BGLAP) and collagen 1A1 (COL1A1) mRNA levels in primary human osteoblasts from two independent donors, relative to TBP. Jurkat cells served as a negative control. (B) qPCR analysis of genes encoding alkaline phosphatase (akp2) and osteocalcin (bglap) 96h after induction of osteoblast differentiation (right). Error bars indicate ±SEM of 3 independent experiments in triplicate ***, P ≤ 0.001 using unpaired student's t test. (C) Alkaline phosphatase substrate staining 96h after induction of osteoblast differentiation. (D) qPCR analysis of rspo1-3 mRNA expression in preosteoblasts and osteoblasts relative to tbp. Error bars indicate ±SEM of 3 independent experiments in triplo. Nd = not determined. (E) Analysis of Wnt activity in TOP.GFP transduced HMCLs treated with R-spondin 2 or low levels of Wnt3a (25ng/mL) in the absence (white) or presence (black) of osteoblast conditioned medium (KS483). Error bars indicate ±SEM of 3 independent experiments in triplicate ***, P ≤ 0.001 using one-way ANOVA with Bonferroni correction.
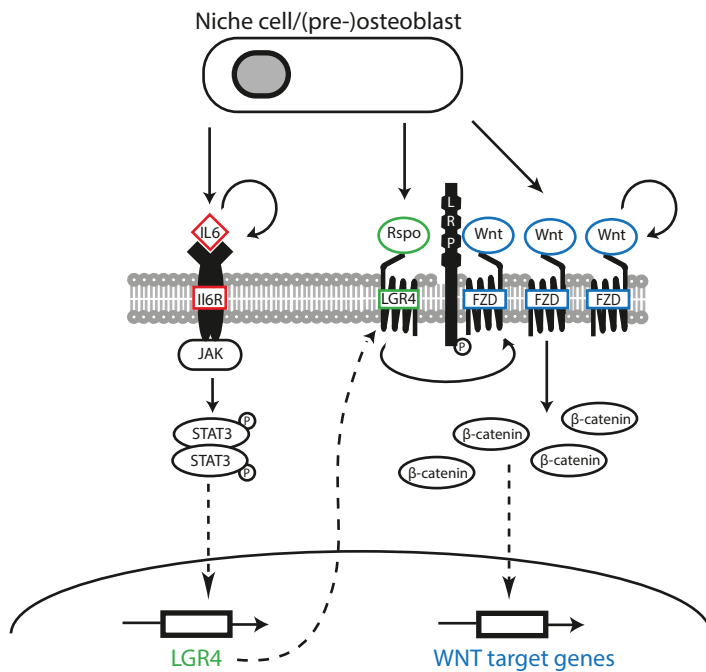
Supplementary figure 8. Model for LGR4/R-spondin mediated Wnt signaling in MM cells. Activation of STAT3 signaling via auto- and/or paracrine IL-6 signaling mediates expression of LGR4, which allows MM cells to hijack (pre) osteoblast derived R-spondins, resulting in Wnt receptor stabilization and sensitization to both auto- and paracrine produced Wnt ligands.

Table S1. Primer sequences

Target	Forward	Reverse
TBP	CCCATGACTCCCATGACC	TTTACAACCAAGATTCACTGTGG
LGR4	CTGAAAGAAGCCTTAGCAGCA	GAGTCACAACCCCAAAATGC
LGR5	CTCCCAGGTCTGGTGTGTTG	GAGGTCTAGGTAGGAGGTGAAG
LGR6	GAGATGGAGGACTCAAAGCCAC	AGTCCATTGCAGAGCACGGAGA
RSPO1	GCTCTGACACCAAGGAGACC	CAGGTTCCTGTTGGCATTCT
RSPO2	GAAACCAGAACACGGCAAAT	TTCGCCTTTGGTGTTCTCTT
RSPO3	ACACCTTGGAAAGTGCCTTG	TTTTTCCCTTCTTCGTGCAT
RSPO4	GACTGTCCCCCTGGGTACTT	ATGCAGAAGTCCTGGCTGAA
ALPL	CTATCCTGGCTCCGTGCTC	GCTGGCAGTGGTCAGATGTT
BGLAP	CTCACACTCCTCGCCCTATT	TTGGACACAAAGGCTGCAC
COL1A1	AAGAGGAAGGCCAAGTCGAG	CACACGTCTCGGTCATGGTA
rspo1	AGACCCGCAAGTGTACCG	GCTCCTTGCTGTTCTTCCTG
rspo2	GGAGTCCAGGAGATGCAAGA	CTTGGGCTCTCTCAATCAGC
rspo3	GTACAAAGAAAGAAGTGTTCAAAGG	GCTGTCAGAGGAGGAGCTTG
akp2	GGATAACGAGATGCCACC	CATCCAGTTCGTATTCCAC
bglap	CAATAAGGTAGTGAACAGACT	CTGGTCTGATAGCTCGTCAC

2